Journal of Macromolecular Science, Part B
Publication details, including instructions for authors and subscription information:
http://www.informaworld.com/smpp/title~content=t713375300

Morphology, Crystallization, and Melting of Single Crystals and Thin Films of Star-branched Polyesters with Poly(-caprolactone) Arms as Revealed by Atomic Force Microscopy

E. Núñez [a]; G. J. Vancso [b]; U. W. Gedde [a]
[a] Fibre and Polymer Technology, School of Chemical Science and Engineering, Royal Institute of Technology, Stockholm, Sweden [b] Materials Science and Technology of Polymers, University of Twente, Enschede, The Netherlands

Online Publication Date: 01 May 2008

To cite this Article Núñez, E., Vancso, G. J. and Gedde, U. W.(2008)'Morphology, Crystallization, and Melting of Single Crystals and Thin Films of Star-branched Polyesters with Poly(-caprolactone) Arms as Revealed by Atomic Force Microscopy',Journal of Macromolecular Science, Part B,47:3,589 — 607

To link to this Article: DOI: 10.1080/00222340801955636

URL: http://dx.doi.org/10.1080/00222340801955636

Journal of Macromolecular Science®, Part B: Physics, 47:589–607, 2008

ISSN 0022-2348 print/1525-609X online
DOI: 10.1080/00222340801955636

Morphology, Crystallization, and Melting of Single Crystals and Thin Films of Star-branched Polyesters with Poly(ε-caprolactone) Arms as Revealed by Atomic Force Microscopy

E. NÚÑEZ,[1] G. J. VANCSO,[2] AND U. W. GEDDE[1]

[1]Fibre and Polymer Technology, School of Chemical Science and Engineering, Royal Institute of Technology, Stockholm, Sweden
[2]Materials Science and Technology of Polymers, University of Twente, Enschede, The Netherlands

*The morphology and thermal stability of different sectors in solution- and melt-grown crystals of star-branched polyesters with poly(ε-caprolactone) (PCL) arms, and of a reference linear PCL, have been studied by tapping-mode atomic-force microscopy (AFM). Real-time monitoring of melt-crystallization in thin films of star-branched and linear PCL has been performed using hot-stage AFM. A striated fold surface was observed in both solution- and melt-grown crystals of both star-branched and linear PCL. The presence of striations in the melt-grown crystals proved that this structure was genuine and not due to the collapse of tent-shaped crystals. The crystals of the star-branched polymers had smoother fold surfaces, which can be explained by the presence of dendritic cores close to the fold surfaces. The single crystals of linear PCL grown from solution showed earlier melting in the {100} sectors than in the {110} sectors, whereas no such sectorial dependence of the melting was found in the solution-grown crystals of the star-branched polymers. The proximity of the dendritic cores to the fold surface yields at least one amorphous PCL repeating unit next to the dendritic core and more nonadjacent and less sharp chain folding than in linear PCL single crystals; this evidently erased the difference in thermal stability between the {110} and {100} sectors. Melt-crystallization in thin polymer films at 53–55°C showed 4 times faster crystal growth along **b** than along **a**, and more irregular crystals with niches on the lateral faces in star-branched PCL than in linear PCL. Crystal growth rate was strictly constant with time. Multilayer crystals with central screw dislocation (growing with or without reorientation of the **b**–axis) and twisting were observed in both classes of polymers.*

Keywords star-branched polyesters, atomic-force microscopy, solution-grown crystals, real-time monitoring, melt-crystallization, melting

Received 7 December 2007; Accepted 20 December 2007.
Address correspondence to U. W. Gedde, Fibre and Polymer Technology, School of Chemical Science and Engineering, Royal Institute of Technology, SE-100 44 Stockholm, Sweden. E-mail: gedde@polymer.kth.se

Introduction

The crystallizable chain segments of the star-branched polymer molecules used in this study are fixed at one end by a dendritic core moiety whereas the other end is free to move. The interest in these polymers was to some extent driven by ongoing research on the possible existence of metastable phases at the early stages of polymer crystallization.[1–5] In these polymers, crystal rearrangement due to annealing is retarded, giving more time to study the materials in their early crystallization stages. The crystallization and melting behavior of star-branched polyesters with crystallizable poly(ε-caprolactone) (PCL) arms have been reported in three previous publications.[6–8] The dendritic cores have a pronounced effect on the crystallization of the linear PCL arms attached to them: slower crystal rearrangement,[6] higher equilibrium melting point,[6] higher fold surface free energy,[7] moderately lower crystallinity,[6] and a greater tendency to form spherulites in comparison with linear PCL.[7] The crystal phase after complete crystallization was however the same for both types of PCL.[6] A detailed analysis of crystallinity data showed that the crystallinity depression, expressed in the number of PCL repeating units (Δn) per PCL arm of the star-branched polymers with respect to linear PCL, is given by:[6]

$$\Delta n = \Delta n_0 + Cn \tag{1}$$

where Δn_0 is a term independent of the length of the crystallizing PCL arm, C is a factor that expresses the depression in crystallinity with increasing length of the PCL arm, and n is the number of repeating units in the PCL arm. Star-branched polymers with dendrimer or dendron cores obeyed Eq. (1) with $\Delta n_0 = 1$ and $C = 0.08$, whereas star-branched polymers with hyperbranched cores showed $\Delta n_0 \approx 5$.[6] These data suggest that PCL chains attached to cores with well-defined structures (dendrimer or dendron) crystallize with the dendritic cores only one PCL repeating unit away from the fold surface ($\Delta n_0 = 1$) and the positive C-value suggests that the folds are less sharp due to the presence of dendritic cores close to the crystal interface. The higher Δn_0 value obtained for polymers with hyperbranched cores seems logical in view of their irregular structure. The placement of dendritic cores in the vicinity of the crystal interface influences the fold surface structure; the possibility of major crystal rearrangement and the presence of a significant cilia phase during crystal growth causing diverging crystal lamellae from lamellar branch points and consequent spherulite formation.[6–8] The attachment of the many crystallizable chains to a single core reduces melt entropy, and this is the major reason for the observed higher equilibrium melting point of star-branched PCL than of linear PCL.[6] This paper, which is a continuation of the previously reported studies,[6–8] addresses the following questions:

i. Solution-grown single crystals of linear PCL showed striations according to transmission electron microscopy (TEM).[8] This structural feature was not detected by TEM in the crystals of star-branched PCL.[8] The open question was whether this feature is absent in the star-branched polymer crystals. Do melt-grown crystals display striations? What is the effect of crystallization temperature on the periodicity of the striated structure?
ii. What is the nature of the fold surface in different sectors of the single crystals of the star-branched polymers and how does it differ from that in single crystals based on linear PCL? What is the thermal stability of different crystal sectors in single crystals of star-branched and linear PCL?

iii. What is the lateral habit of melt-grown crystals based on star-branched PCL? Single crystals of star-branched PCL grown from solution at temperatures between 30°C and 40°C were in many cases more extended along the crystallographic **a**−axis than along the **b**−axis and the lateral faces contained many niches.[8]

This paper presents data obtained by tapping-mode atomic-force microscopy (AFM) for the morphology, crystallization, and melting behavior of solution-grown single crystals and thin films of star-branched PCL and reference linear PCL. Atomic-force microscopy provides surface imaging with quantitative height data essential for assessing crystal thickness and, most important in this study, for obtaining information about the striated structures. Atomic-force microscopy is able to monitor hot-stage in-situ melting and crystallization at controlled temperatures. Hobbs et al.[9] were the first to perform an in-situ study at room temperature, whereas Pearce and Vancso[10] reported the first hot-stage in-situ observation of melting and crystallization.

This study has confirmed that both solution- and melt-grown crystals of both linear and star-branched PCL exhibited striated surfaces. The observation of striations in crystals growing from the melt indicates that this feature is not due to a collapse of tent-shaped crystals. The paper also presents data on melting behavior, confirming differences in the fold surface structure of the solution-grown single crystals between star-branched and linear PCL. Real-time monitoring of melt crystallization provided a wealth of information about the morphological features of the crystallization of star-branched polymers. The newly obtained data combined with earlier reported data for solution-grown single crystals[8] conform to a trend with increasing crystal shape anisotropy, expressed as the ratio of the crystal length along **b** to that along **a**, with increasing crystallization temperature.

Experimental

Materials

The star-branched polymers consisted of PCL grafted to dendritic hydroxyl-functional cores. The cores used were a third-generation hyperbranched polyester with approximately 32 terminal hydroxyl groups (Boltorn, Perstorp AB, Sweden) and a third-generation dendrimer with 24 hydroxyl groups. The synthesis and characterization of the star-branched polymers have been described earlier.[11,12] A linear PCL sample with the trade name Tone P300 purchased from Union Carbide, USA, was studied as received. Molecular structure data from the polymers studied are presented in Table 1. The structures of the star-branched polymers are sketched in Fig. 1.

There is a sizeable difference in the degree of polymerization (*DP*) of the crystallizable PCL units of the star-branched polymers ($DP = 51$) and the linear PCL ($DP = 117$). Earlier studies[6−8] showed, however, that the morphological effect of this difference in molar mass for linear PCL is relatively small: Single crystals of linear PCL's with *DP* of 39 and 117 grown from solution at 35−40°C showed the same lateral habit.[8] These linear polymers showed the same superstructural transitions as a function of crystallization temperature; the transition from irregular spherulites to axialites appeared at ca. 4°C lower temperature in the lower molar mass polymer.[7] The degree of crystallinity for samples crystallized at 10°C/min was 0.70 for a PCL with $DP = 50$ (value obtained by interpolation) and 0.65 for PCL_{117}.[6] The fold surface free energy (σ) values obtained from crystallization kinetics data were 60−80 mJ/m^2 ($DP = 50$) and 105 ± 15 mJ/m^2

Table 1
Nomenclature and characteristics of the polymers studied

Sample code	Core	M^a_{core}	n^b_{arms}	n^c
PCL_{117}	None	0	1	117 (1.4)
D_{51}	3rd generation dendrimer	3.0	24	51 (1.3)
HB_{51}	3rd generation hyperbranched	3.6	32	51 (1.3)

[a]Molar mass in kg mol^{-1} of core calculated theoretically from the chemical formula.
[b]Number of PCL arms attached to each core.
[c]Number average of the degree of polymerization of the PCL arms (n) obtained by H-NMR.[11] The values within parentheses show the polydispersity ($\bar{M}_W/\bar{M}_n$) obtained by size-exclusion chromatography applying the universal calibration procedure. These values presented for the star-branched polymers have been estimated from data for linear PCL polymerized under similar conditions.

($DP = 117$).[7] The σ-values of the polymers used in this study were almost the same: 105 ± 15 mJ/m^2 (PCL_{117}) and 100 ± 15 mJ/m^2 (D_{51} and HB_{51}), which is in the proximity of the 'polymeric regime.' This study thus properly addressed the effect of molecular architecture on the fold surface structure and the other issues raised in the previous discussion.

Preparation of Single Crystals

Single crystals were grown from dilute solution according to the self-seeding method.[13] The polymer was dissolved in *n*-hexanol or *n*-butanol to obtain solutions with 0.05 wt.% of polymer. The solutions were transferred to vials immersed in an oil bath, which was set at either 35°C or 40°C, and allowed to crystallize at this temperature overnight. After crystallization, the vials were rapidly transferred to an oil bath set at the dissolution temperature, which ranged from 42°C to 59°C. After keeping the vials at these temperatures for a

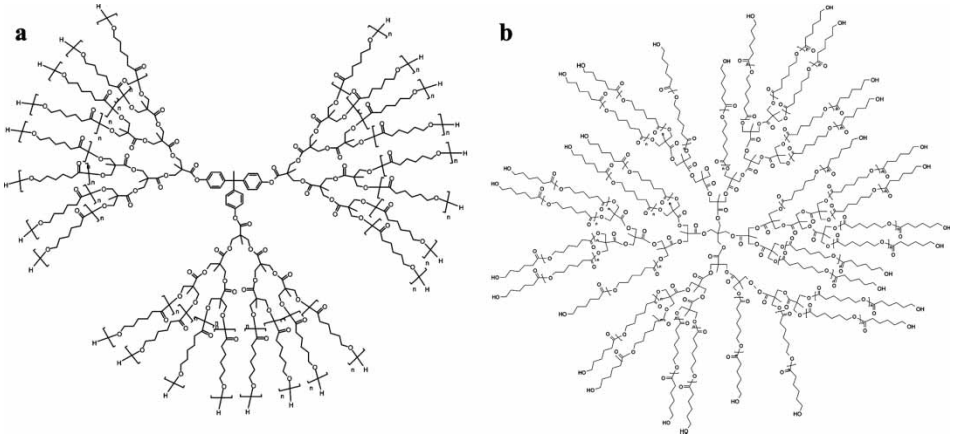

Figure 1. Chemical structures of the star-branched polymers studied: (a) D_n (star-branched PCL with dendrimer core, $n = 14$ and 51); (b) HB_n (star-branched PCL with hyperbranched core, $n = 51$).

few minutes they were immediately transferred back to the bath at the crystallization temperature. The process was repeated thrice. The suspensions were finally allowed to cool to room temperature without filtration. The crystal suspensions were dropped onto glass substrates and allowed to dry prior to microscopic observation.

Preparation of Thin-film Samples

Films with a thickness of ca. 200 nm were prepared by spin-coating a solution of the polymer in chloroform (5 mg polymer per ml solvent) onto cleaned glass surfaces at 3000 rpm for 30 s. The glass substrates had been cleaned by immersion in chloroform and ethanol and after drying by exposure to oxygen plasma for 10 min.

Atomic-force Microscopy (AFM)

The AFM experiments were performed at ambient conditions using a Multimode microscope with NanoScope III controller (Veeco). The instrument was equipped with a J-scanner. The maximum scan size was 100 μm^2. Commercially available Si-cantilevers (NANOSENSORS^{TM}) with resonance frequency of 204–497 kHz and force constants of 10–130 N/m, according to the manufacturer, were used. Measurements were carried out in the tapping mode, using always the largest set-point ratio to minimize interactions between the tip and the sample. This was particularly important in the real-time study of crystallization, because the tip may induce crystallization by shear forces in the contact mode.[14] A high-temperature accessory provided by Veeco was used. It enabled heating from ambient to 250°C. Height, amplitude, and phase images were acquired simultaneously.

The high temperature experiments were carried out as follows: The sample stage and tip were heated from room temperature to melting temperature in steps of 1–5°C. The tip was always withdrawn from the sample during heating. Tip engagement was executed only after the selected temperature had been reached and remained stable. Images were acquired under isothermal conditions. The larger temperature jumps were used at the lowest temperatures. When the first morphological changes were observed, the temperature jumps were decreased. Real-time monitoring of crystallization was performed under isothermal conditions after cooling the samples from the melt to the crystallization temperature.

Results and Discussion

Striated Fold Surfaces in Solution- and Melt-grown Crystals

Figures 2 and 3 display images of a 12 nm-thick single crystal grown from a dilute *n*-hexanol solution of PCL_{117} at 40°C. The lateral habit of solution-grown single crystals of linear and star-branched PCL, including the crystallographic assignment of the lateral faces was reported in a previous paper.[8] However, a few important key features are repeated here as a background. The crystallographic **b**-axis is parallel to the long-axis of the crystal shown in Fig. 2a. These crystals showed six sectors: four {110} sectors and two {100} sectors. The crystal displayed in Figs. 2a and b shows an outer highly irregular crystal layer with deep niches in the {110} sectors. It is believed that the external part of the crystal showing irregular growth faces was formed during the cooling of the solution to room temperature.

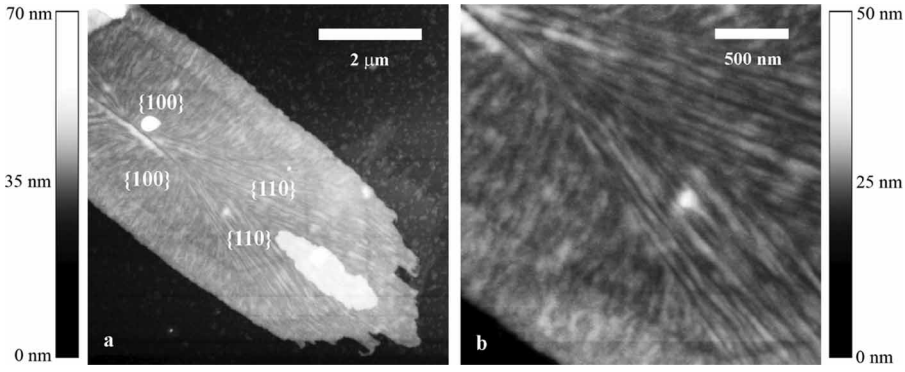

Figure 2. Height AFM images (Fig. 2b is a magnification of a part of the single crystal shown in Fig. 2a) of a single crystal of PCL_{117} grown from a dilute *n*-hexanol solution at 40°C.

Sectorization is evident in the single crystals displayed in Figs. 2 and 3. Sectors in single crystals can be revealed by the use of decoration techniques.[15] However, in the present study the different crystal sectors were visible without such treatment. Striations running from the centre and outwards gave a height contrast, which revealed the different sectors. Figures 2a and b show striations in the {110} sectors running parallel to the boundaries between the {110} and {100} sectors. The angle formed between the striations in the {110} sectors and the corresponding growth faces was not necessarily 90°, as was reported earlier by Iwata et al.[16] The value of this angle depends on the relative growth rates of the different sectors which, according to Núñez and Gedde,[8] vary depending on polymer structure and crystallization temperature; the latter was further confirmed by data presented in the final section of Results and Discussion. The striations appeared in the height images (Figs. 2a, b, and 3a), phase images (Fig. 3b), and amplitude images (not shown). A close examination of the height and phase images presented in Figs. 3a and b confirms that they represent the same structure. The phase image structure is, generally speaking, due to spatial variation of the viscoelastic

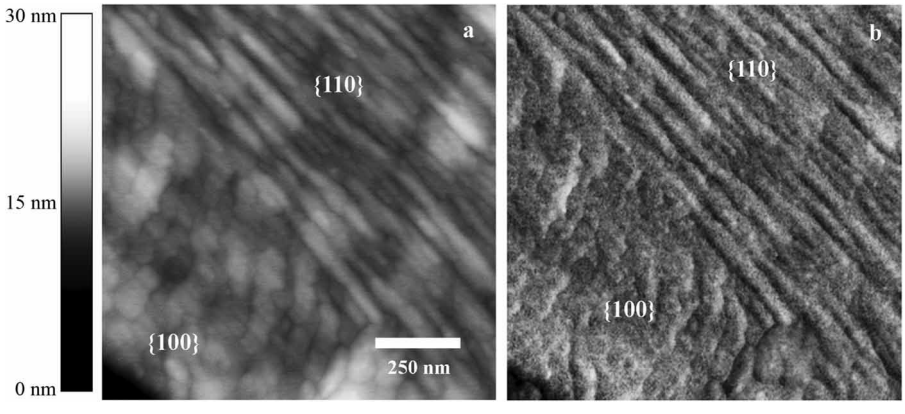

Figure 3. (a) Height and (b) phase AFM images of a single crystal of PCL_{117} grown from a dilute *n*-hexanol solution at 40°C. The full data scale for the phase image was 20°.

properties. The resemblance of height and phase images thus indicates that viscoelastic properties and thickness are correlated.

The striations were more pronounced and continuous in the {110} sectors than in the {100} sectors (Figs. 2 and 3); the striations in the latter sectors grew along the normal to the growth face and exhibited a more granular morphology. The striations observed in the {110} sectors in Figs. 2 and 3 were 55 to 60 nm wide, essentially continuous through the whole sector and ca. 1.7 nm high. The dimensions of the granules observed in the striations of the {100} sectors were of the order of 50–60 nm (width) and 30 nm (length) and approximately 1.7 nm high (Figs. 3a and b). Another remarkable feature is the continuity of the striations through the observed boundary that separates areas of the crystals corresponding to consecutive growth stages (Fig. 2). The lamellar thickness was lower in the peripheral region, which indicates that the overgrowth occurred during the cooling of the solution to room temperature. The striations ran continuously through the boundary between the thick and thin crystal regions. The periodicity of the striations was approximately the same in both regions of different crystal thickness (Fig. 2b). It is important to point out that the striated fold surfaces of solution-grown crystals of linear PCL have been reported earlier.[8,16] However, the detailed information about the height of the modulation obtained by AFM is new.

Figures 4a and b show amplitude and phase images of single crystals of HB_{51} grown from dilute *n*-butanol and *n*-hexanol solutions respectively at 40°C. The height images just barely revealed the striations, indicating that the height amplitude was smaller than in the case of linear PCL. The striations in the different growth sectors were visible in the single crystals of the star-branched polymers but they were less well-defined and the surfaces of these crystals appeared more granular than those of linear PCL. The orientation of the striations with regard to the crystallographic axes and the overall continuous character from the centre to the crystal periphery were essentially the same for the star-branched polymer as for linear PCL (Figs. 2 and 4). The widths of the striations, most clearly seen in Fig. 4b, were 50 ± 20 nm. It is important to point out that the other star-branched polymer studied (D_{51}) also displayed solution-grown crystals with striations on the fold surfaces.

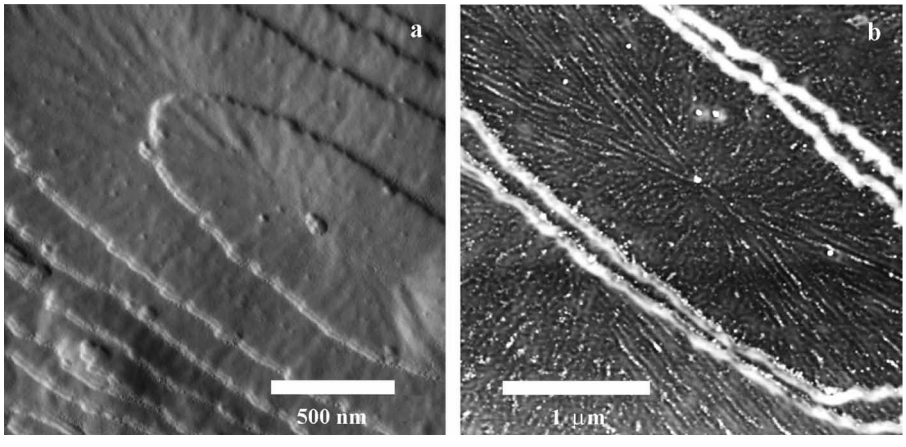

Figure 4. (a) Amplitude AFM image of single crystals of HB_{51} grown from a dilute *n*-butanol solution at 40°C. Full data scale = 200 mV. (b) Phase AFM image of a single crystal of HB_{51} grown from a dilute *n*-hexanol solution at 40°C. Full data scale = 15°.

Striations were also observed in the fold surfaces of melt-grown crystals of both linear and star-branched PCL (Figs. 5a and b). These micrographs were from in-situ crystallization experiments and the striations were formed at the crystallization temperature (53°C and 55°C, respectively). The crystal terraces displayed in Fig. 5a (PCL_{117}) show some very interesting features. The more developed layers show pronounced striations whereas the upper, more newly formed layers just barely show striations. The widths of the striations in the linear PCL sample were 50–100 nm; i.e., slightly larger than was observed in the solution-grown crystals, The orientation of the striations was essentially the same in the melt-grown crystals as in the solution-grown crystals (Figs. 2 and 5a). The more-developed bottom layers of the terraces of the melt-crystallized D_{51} sample showed vague striations with a width of 100–150 nm (Fig. 5b). The top layer of the terraces showed a very distinct, remarkably different structure. We have currently no explanation for this unique structure. The observation of striated melt-grown crystals is not new. Taguchi et al.[17] reported undulated melt-grown crystals of isotactic polystyrene revealed by AFM. They determined the height amplitude to about 1 nm and found also that the periodicity of the undulations (striations) increased with increasing crystal thickness; i.e., with increasing crystallization temperature.

In conclusion, the striated structures on the fold surfaces are a general feature common to both linear and star-branched PCL and also general with regard to the source medium of the crystals; i.e., solution or melt. The striations were visible in height, amplitude, and phase images and comparison of these images reveals that they originated from the same basic structure. The striations appeared as a regular height variation in the fold surface with ca. 1.7 nm amplitude for solution-grown crystals of linear PCL or less for star-branched PCL. The smaller height amplitude and the more vague character of the striation in star-branched PCL crystals than in linear PCL crystals can be explained by two different effects: (i) The dendritic core moieties cover the fold surface in a octopus-like structure and, in addition, the degree of crystallinity of the PCL component is lower in HB_{51} and D_{51} than in PCL_{117}. Núñez et al.[6] provided the following data on mass crystallinity of melt-crystallized samples: 0.65 (PCL_{117}), 0.56 (HB_{51}), and 0.63 (D_{51}). Hence, the amorphous layer, consisting of the dendritic core moieties and

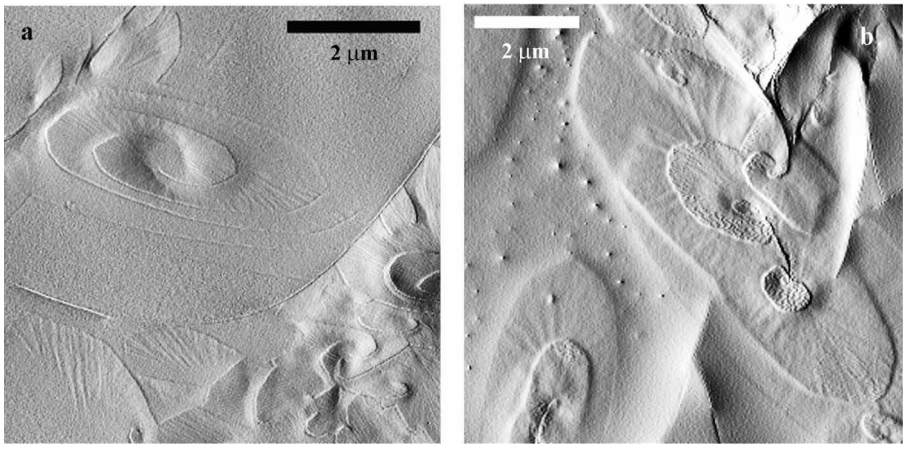

Figure 5. Amplitude AFM images of thin-film samples: (a) PCL_{117} crystallizing at 55°C; (b) D_{51} crystallizing at 53°C. Full data scale = 50 mV.

amorphous PCL units, should be thicker on the single crystals based on star-branched PCL than on those of linear PCL and this is expected to smear out the crystal striations as observed by tapping mode AFM. (ii) The dendritic core modifies the fold surface structure changing the stress build-up possibly responsible for the striations; Taguchi et al.[17] proposed that the stress of fold surfaces makes a flat crystal elastically unstable to cause a buckling deformation during crystallization. Common to all studied systems (solution- and melt-grown crystals of linear and star-branched PCL) was the distinct orientation of the striations along the boundary between the {110} and {100} sectors in the {110} sectors and along (100) in the {100} sectors. The sectorial feature of the striations together with their regular appearance on the fold surfaces strongly suggests they originate from the fold structure. Another important finding was the presence of striations in melt-grown crystals, which indicates that the striations were formed during crystallization and not as the result of collapse of a nonplanar (tent-like) crystal as has been suggested by Pouget et al.[18] An indication that the formation of the striation is a gradual process is presented in Fig. 5a: The striations are more developed in 'older' bottom layers of terrace crystal than in the 'young' top layer. The presented data for PCL are in general agreement with the findings of Taguchi et al.[17] on melt-grown crystals of isotactic polystyrene. Taguchi et al.[17] reported that the spacing of the striations was proportional to the reciprocal degree of supercooling; i.e., to crystal thickness. The data presented are in most respects consistent with this empirical finding. However, the fact that the spacing of the striations remained intact crossing the boundary between crystal domains of different crystal thickness (see Fig. 2a) is not in accordance with the data presented by Taguchi.[17]

Structural Changes of Solution-grown Single Crystals on Heating

Figure 6 shows the effect of heating on solution-grown single crystal of PCL_{117}. The crystals were 9 nm thick with flat {110} faces and slightly rounded {100} faces before heating (Fig. 6a). No morphological changes were observed at temperatures below 55°C. At 55°C, the first morphological changes were observed at the edges of the single crystal as indicated with the arrows in Fig. 6b. Ridges were formed running parallel to the striations towards the center of the crystal, forming patches of thicker (14–16 nm) material. Similar behavior has been reported for single crystals of polyethylene,[19] *n*-alkanes,[20] poly(ethylene oxide),[21] and poly(*l*-lactic acid).[22] The less-confined crystal edges are expected to be thermally less stable than the central region of the crystal.[19–22] Immediately after the appearance of the ridges, significant restructuration was observed in some regions within the {100} sectors (Figs. 6b and c). Holes were formed, supplying material to the region undergoing thickening. The average thickness of the thickened regions was 18–20 nm, but regions with thicknesses between 25 and 30 nm were also observed as indicated by the dark arrows in Fig. 6c. The white arrow in Fig. 6c marks a region of lower thickness (6 nm). It is important to note that the {110} sectors remained essentially unchanged at 55°C. After 17 min at 56°C, significant structural changes had also occurred within the {110} sectors (Fig. 6d). A difference in thermal stability between the different sectors has previously been reported for single crystals of polyethylene.[19,23,24] The behavior of solution-grown crystals of linear PCL thus resembles that of polyethylene. The different fold structure of the different sectors may have an effect on the entropy of melting or have a slight effect on the packing of the crystal stems thus affecting the enthalpy of melting.

Figure 7 shows the thermally induced changes in a 9 nm-thick single crystal of HB_{51}. No morphological changes were detected at temperatures below 48°C and the crystal

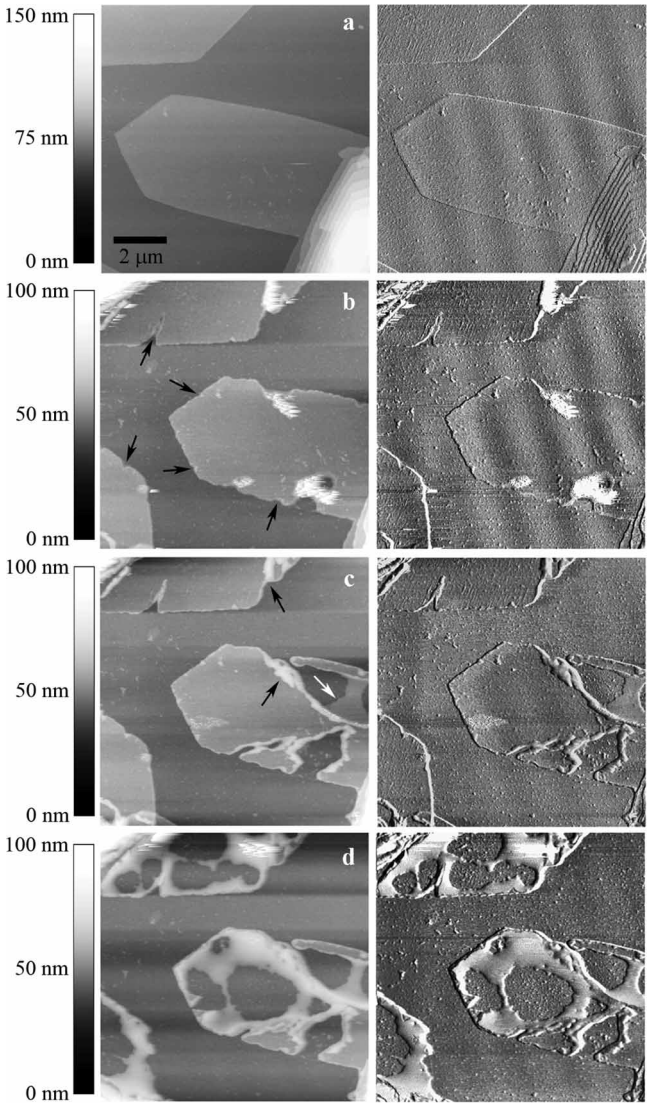

Figure 6. Height (left-hand column) and phase (right-hand column; full data scale = 25°) AFM images of PCL_{117} single crystals taken at different temperatures after different annealing times: (a) 23°C; (b) 55°C after 17 min; (c) 55°C after 60 min; (d) 56°C after 17 min.

resembled the initial structure displayed in Fig. 7a. The crystal edges started to rearrange at 48°C (Fig. 7b). The arrows in Fig. 7b mark regions of reduced thickness, 5 nm. This not generally observed and unexpected event is most probably due to flattening of height images leading to certain distortions. The crystal that was heated further in temperature steps of 1–3°C to 57°C showed only minor changes in the structure of the crystal edges, and no morphological change was observed in the central regions of the crystal (Fig. 7c). In the phase image of Fig. 7c, the white lines define the demarcation between a single crystal layer and a second crystal layer referred to as an 'overgrowth.' The rearrangement observed at temperatures between 57 and 59°C (the images are not

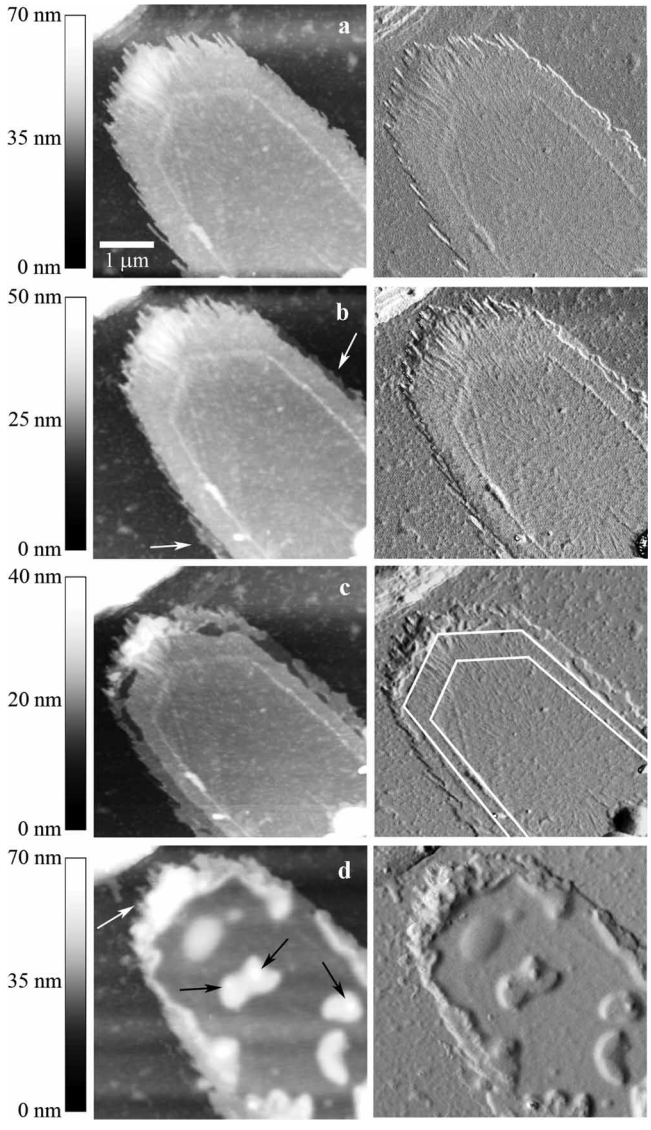

Figure 7. Height (left-hand column) and phase (right-hand column; full data scale = 25°) AFM images of a HB_{51} single crystal at (a) 23°C; (b) 48°C after 8.5 min; (c) 57°C after 8.5 min; (d) 60°C after 8.5 min.

shown due to their inferior quality) involved only the area corresponding to the crystal overgrowth; the latter was probably formed by polymer crystallized at a higher degree of supercooling than the central crystal area. At 60°C, significant structural changes were observed in all sectors of the crystal (Fig. 7d). The different sectors in the star-branched PCL single crystals thus showed similar thermal stability. No holes were generated by the thermal treatment, which was clearly different from the behavior of the single crystal of linear PCL (Fig. 6d). Some areas of the crystal; i.e., the edges and some 'islands' in the centre of the crystal underwent thickening. The average thickness

in the thickened regions was 16–19 nm, but in some regions, indicated by the black arrows, it was 26–28 nm. In the region indicated by the white arrow, the thickness was 37–40 nm. The large dark regions in the micrograph shown in Fig. 7d indicated, however, that most regions in the crystal showed a decrease in thickness, finally approaching a thickness of ca. 5 nm. The presence of holes in the annealed linear PCL single crystals is caused by the difference in surface free energy between the fold surface (high value) and the lateral surfaces (low value).[6,7] Nunez et al.[7] showed that the surface energetics of the star-branched PCL single crystals is similar to that of linear PCL single crystals. The reason for the absence of holes in the annealed star-branched PCL is thus not that the thermodynamic strive toward a smaller the fold surface area is lacking but rather that the process is kinetically hindered by the dendritic cores.

The difference in thermal stability of the different sectors in the linear PCL single crystals is already known. The new finding is the uniformity in thermal stability of different crystal sectors of the star-branched PCL single crystals, which indicates that the presence of the dendritic cores has an effect on the fold surface structure. As previously discussed, the proximity of the dendritic cores to the fold surface has two effects: (i) one PCL repeating unit next to the dendritic core is amorphous; (ii) chain folding becomes less sharp and possibly less adjacent than in linear PCL single crystals. The difference between the fold structures in the {110} and {100} sectors thus becomes insignificant resulting in the almost simultaneous melting of the different sectors of the single crystals of the star-branched PCL sample.

Melt-crystallization of Thin-film Samples: Lateral Habit and Crystal Growth Rate

The principal issues dealt with in this section are the lateral habit of melt-grown crystals of star-branched PCL and the characteristics of crystal growth during isothermal conditions. The problem of identifying the crystallographic axes of a given crystal is an important factor that can lead to misinterpretation of crystal growth rate data obtained by AFM. This problem was addressed by comparing linear growth rate data of an ensemble of crystals, some with known crystallographic axes orientations. Figures 8 and 9 present a series of micrographs taken after different periods of time under isothermal conditions at 53°C and 55°C respectively, showing the growth of crystals from the molten state in thin-film samples of PCL_{117} and D_{51}. Both polymer samples initially showed only edge-on lamellae (Figs. 8a and 9a). This suggests that crystallization was initiated at the substrate boundary with the chain (**c**) axis parallel to the substrate plane. It is not possible on the basis of the micrographs to assess the orientation of crystallographic axes **a** and **b** in the edge-on lamellae. As crystallization proceeded, flat-on crystal lamellae became visible (Figs. 8b–d and 9b–d). The growth faces in the flat-on lamellae in the linear PCL thin film are clearly revealed in Fig. 8d (F1): the crystallographic **a**– and **b**–axes are almost horizontal, the {110} growth faces are relatively flat, the apex angle is approximately 125° and the {100} faces show curvature. The aspect ratio, defined as the crystal length along **b** (l_b)/crystal length along **a** (l_a), is, according to this micrograph, approximately 4. Figures 9c and d display a flat-on lamella (F2) at different growth stages in the D_{51} thin film. The crystallographic axes **a** and **b** (indicated in Fig. 9c) are readily identified from the lateral habit, which is similar but not identical to that of the linear PCL crystal (Fig. 8d). The {100} faces showed more curvature in the crystal of the star-branched PCL than in the linear PCL crystal. A close examination of crystal F2 in Fig. 9d indicated the presence of shallow niches at the lateral faces. Solution-grown single crystals formed at 30–40°C displayed a large

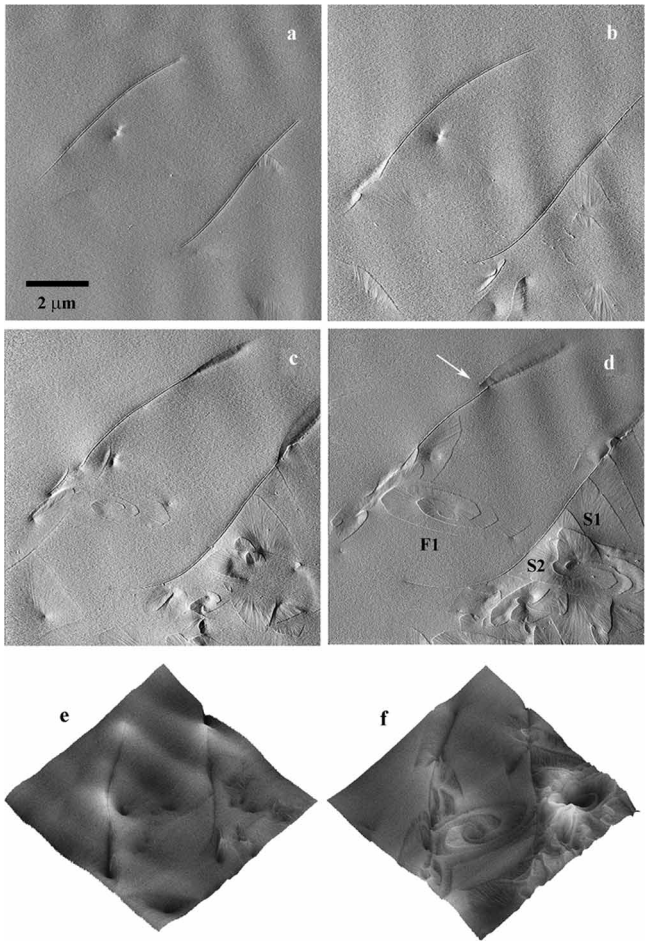

Figure 8. Amplitude AFM images of a thin film of PCL_{117} crystallizing at 55°C after different periods of time: (a) 111 min; (b) 145 min; (c) 195 min; and (d) 229 min. (e and f) Height surface plots (the scanned area is 10×10 $(\mu m)^2$) of the same sample after (e) 195 min and (f) 290 min. The full data scale for the amplitude images was 30 mV.

number of niches on the lateral faces.[8] The aspect ratio (l_b/l_a) for the single crystals of both linear PCL and star-branched PCL was ca. 4.

Figure 10 shows the size of the crystal lamellae along the crystallographic **a** and **b** axes plotted against time for a flat-on lamella of D_{51} crystallizing at 53°C. The growth rate was strictly constant. This is in accordance with other studies.[10,25,26] Variations in the crystal growth rates have been observed but only over very short length and time scales.[27] Such short length and time scales were not resolved in the present study. The growth rates obtained from the data presented in Fig. 10 were 0.018 μm/min (along **a**; v_a) and 0.076 μm/min (along **b**; v_b). These growth rates thus correspond to a crystal aspect ratio (l_b/l_a) of 4.2. Núñez and Gedde[8] showed that solution-grown single crystals grown at 30–40°C had crystal aspect ratios (l_b/l_a) between 1.5 and 1.8 for linear PCL and between 0.8 and 1.3 for star-branched PCL (DP for PCL arms was between 40 and 80). Thus, the crystal aspect ratio (l_b/l_a) increases with increasing

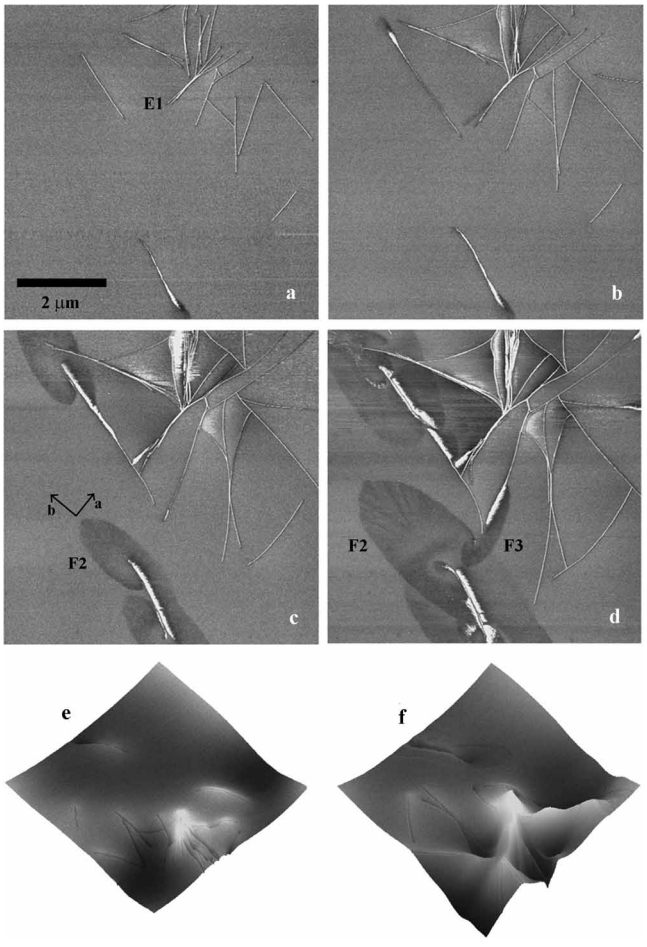

Figure 9. Phase AFM images of a thin film of D_{51} crystallizing at 53°C after different periods of time: (a) 8.5 min; (b) 17 min; (c) 34 min; and (d) 51 min. (e and f) Height surface plots (the scanned area is 7×7 $(\mu m)^2$) of the same sample crystallizing for (e) 8.5 min and (f) 34 min. The full data scale for the phase images was 30°.

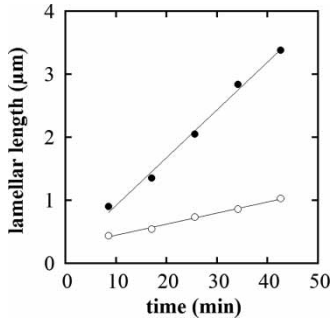

Figure 10. Lamellar length along the **b** (filled symbol) and **a** (open symbol) crystallographic axes of a flat-on lamella in a thin film of D_{51} crystallizing at 53°C. The lines show the linear fits to the experimental data.

crystallization temperature, which is a trend that was established for polyethylene by Organ and Keller.[28] It is important to point out that the data by Organ and Keller showed that lateral habit for this particular polymer was controlled by the absolute temperature rather than by the degree of supercooling. It seems that linear and star-branched PCL follow the same basic principle. Anisotropic crystal growth has been reported for melt-crystallized linear PCL by Beekmans and Vancso,[29] which is in principle agreement with the findings reported in this paper.

The growth rates of the edge-on lamellae showed significant variation between different lamellae. However, the values were always between v_a and v_b. Most of the edge-on lamellae showed a growth rate that was 60–70% of the growth rate along **b**. It is suggested that the growth of the edge-on lamellae was controlled by the growth along **a**. The hypothesis, illustrated in Figs. 11a–c, is that the crystals nucleated at the substrate boundary (Fig. 11a), as has been proposed earlier by Godovsky and Magonov[30] and by Li et al.,[31] and that the crystal grew fastest along **b**. After a

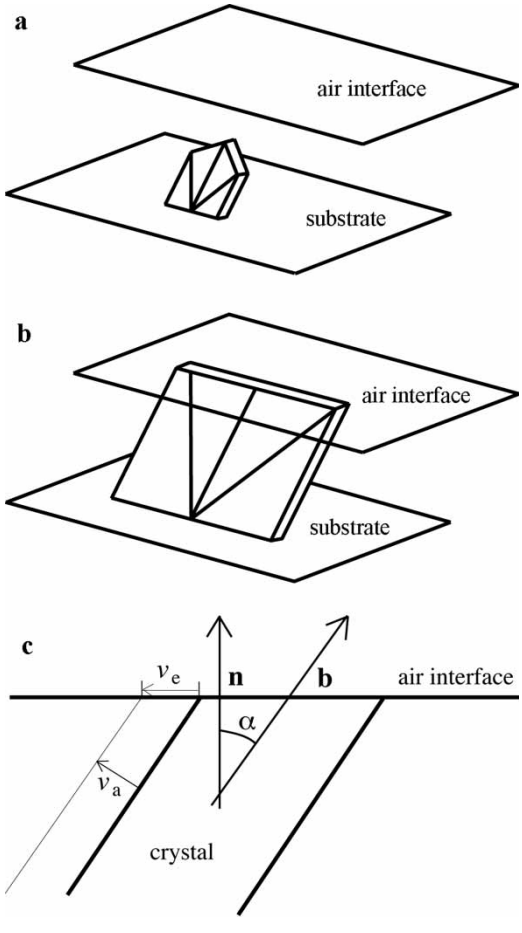

Figure 11. Schematic representation of the growth of a crystal in a thin-film sample: (a) the crystal grows freely in the melt along **a** and **b**; (b) the crystal grows along b after reaching the air interface; (c) measured growth rate (v_e) by crystal growth along **a** (rate v_a). The angle between the crystallographic **b**-axis and the interface normal (**n**) is denoted α.

certain time, the crystal growth boundary, i.e., the two {110} faces, reached the air-interface and the growth along **b** was stopped because of the spatial confinement (Fig. 11b). Hence, the crystal could only grow only along **a** at this stage. The apparent growth rate at the film boundary (v_e) is related to both v_a and the angle (α) between **b** and the normal to the air-interface (Fig. 11c):

$$v_e = \frac{v_a}{\cos \alpha} \tag{2}$$

The most typical growth rates obtained corresponded to an angle, α, between 60 and 70°. The lowest measured growth rate (v_e) was close to v_a, suggesting that the **b**-axis of this crystal was along the normal to the film plane (Fig. 11c).

Two different types of terraced multilayer crystals were observed in the thin film of the linear PCL (Fig. 8d). The terraces indicated by F1 are parts of a simple continuous structure with a central screw dislocation. The different layers have a common **b**-axis. This structure resembles that of the multilayer crystals grown from a dilute solution of this polymer.[8] In the right-hand bottom corner of the same micrograph (Fig. 8d), there are screw dislocations including a number of crystal layers pointing with the **b**-axis in different directions in the plane. Closer examination indicates that there are at least two groups of terraces with crystal layers with common **b**-axis orientations; one of which originated from an edge-on lamella (this group is denoted S1). The other group (denoted S2) has its center in one of the crystal layers of the S1-group from which it may have developed. The angle between the **b**-axes of the two lamellae stacks was approximately 45°. The fact that these multilayer crystals are stacked on top of each other does not mean that they would not form a three-dimensional structure in an unconfined molten phase. The spatial confinement of cilia and other amorphous segments between the crystal layers should produce a splaying structure in the free melt.

Multilayer structures with lamellar branching were also found in a few cases in the edge-on lamellae. On the right-hand side of E1 in Fig. 9a, several branched structures; i.e., one edge-on lamella continued into two diverging edge-on lamellae, appeared in the star-branched polymer film. It should be noted that the view plan is a mixed **ab**-plane. Some of the branched lamellae showed twisting; i.e., a gradual change of the **c**-axis orientation, immediately after the branching point. Twisting of the edge-on lamellae was another noticeable feature. Such structures were found in the linear PCL sample (Fig. 8d; marked with the white arrow) but they were even more frequent in the thin film of the star-branched polymer (Fig. 9d). There are several examples of edge-on lamellae that essentially stopped to grow followed by the growth of a flat-on lamella (Fig. 9c, d; structure marked with F2). Structure F3 in Fig. 9d is another example of similar morphology. The edge-on lamella seems to twist in both these cases and our hypothesis is that the flat-on lamella is the result of a screw dislocation yielding a lamellar branch beneath the air-interface. The branching lamella has to reorient and twist to some extent in a free, unconfined melt. The situation near the air-interface is different. The spatial confinement may lead to a further reorientation of the crystal approaching a flat-on orientation. Kikkawa et al.[32] studied crystallization of PLLA films. They proposed that the flat-on crystals grew from the edge-on crystal from the {001} faces. They assumed that the cilia dangling out from the {001} faces crystallized in the flat-on lamellae. The exact mechanism was not really discussed but two mechanisms seem possible: (1) epitaxy, which in our opinion seems not to be a very feasible mechanism; (2) increase of the equilibrium melting point because of molecular

constrain (lowering of entropy of the cilia). Hence, the driving force for crystallization (effective degree of undercooling) would be increased.

The following main conclusions were drawn from results presented in this section: The anisotropic crystal growth of both linear and star-branched PCL, approximately four times faster along **b** than along **a**, was established on the basis of the growth of flat-on crystal lamellae. This is not a new finding for linear PCL but it has hitherto not been reported for star-branched PCL. A general temperature dependence of the relative growth rates was established based on the new data; i.e., data from melt-crystallization at 53–55°C, and on earlier published data for single crystals grown from solution at 30–40°C. For both classes of polymers, it conforms to the well-known trend: The crystal growth rate ratio (v_b/v_a) increases with increasing temperature. The flat-on crystals observed in the star-branched PCL samples had shallow niches, which is different from the crystals of linear PCL observed; the latter showed smoother lateral faces. This difference was also reported for solution-grown single crystals[8] and was attributed to differences in fold-surface free energy and to the molecularly constrained nature of the star-branched polymers. The presence of screw dislocations and, in the case of an unconfined melt, diverging crystal lamellae were confirmed for both linear and star-branched PCL. It is suggested that the apparently sharp transition from edge-on to flat-on lamella is due to the presence of a screw dislocation beneath the air-interface leading to reorientation and twisting.

Conclusions

Solution- and melt-grown crystals of both linear and star-branched PCL exhibited striated fold surfaces. The orientation of the striations was specific for each crystal sector. The striations were more defined in the crystals of linear PCL, whereas the crystals of the star-branched polymers had smoother fold surfaces. This difference can be attributed to the coverage of the fold surface with dendritic core moieties in the star-branched polymers and to the change of the nature of the fold due to proximity of the dendritic cores to the fold surface. The fact that striations were also found in melt-grown crystal indicate these structures were genuine and not due to the collapse of tent-like crystals. The solution-grown crystals of linear PCL showed earlier melting in the {100} sectors than in the {100} sectors. Similar observations have been reported for other linear polymers such as polyethylene. The star-branched polymers showed melting with no such sectorial preference. This indicates that the structure of the fold surface is changed by the presence of the dendritic cores in the star-branched polymer. Crystallization from the molten state at 53–55°C yielded more irregular crystals (shallow niches on the lateral faces) in the star-branched polymer than in the linear PCL. This finding is consistent with earlier results presented for solution-grown single crystals. The anisotropic crystal growth of both linear and star-branched PCL, strictly constant with time and approximately four times faster along **b** than along **a**, was established on the basis of the growth of flat-on crystal lamellae. By combining these data with earlier data reported for solution-grown crystals, it is shown that the ratio of crystal growth rate along **b** to that along **a** increases with increasing crystallization temperature; this is in accordance with earlier reported data for polyethylene. The crystal growth rate was anisotropic but strictly constant for a given crystallographic direction. However, crystals with different orientations of their crystallographic axes showed significant variations in measured linear growth rates. This demonstrates the importance of assessing the crystallographic axes orientations before determining physically realistic linear growth rates

from AFM micrographs. Multilayer crystal structures with a central screw dislocation and, in the case of an unconfined melt, diverging crystal arms were confirmed for both linear and star-branched PCL.

Acknowledgments

The financial support from the Swedish Research Council (grant no. 5104-20005764/20) is gratefully acknowledged. Thanks are extended to Drs. E. Malmström and H. Claesson, Royal Institute of Technology, for supplying the star-branched polymers. Drs. H. Schönherr and S. Zapotoczny, University of Twente, are acknowledged for valuable experimental advice and scientific discussions.

References

1. Ungar, G.; Rastogi, S. Hexagonal columnar phases in 1,4-trans-polybutadiene: Morphology, chain extension and isothermal phase reversal. Macromolecules **1992**, *25*, 1445–52.
2. Keller, A.; Hikosaka, M.; Rastogi, S.; Toda, A.; Barham, P.J. Approach to the formation and growth of new phase with application to polymer crystallization: effect of finite size, metastability, and Ostwald's rule of stages. J. Mater. Sci. **1994**, *29*, 2579–604.
3. Strobl, G. From the melt via mesomorphic and granular crystalline layers to lamellar crystallites: a major route followed in polymer crystallization. Eur. Phys. J. E: Soft Matter **2000**, *3*, 165–83.
4. Wurm, A.; Soliman, R.; Schick, C. Early stages of polymer crystallization–a dielectric study. Polymer **2003**, *44*, 7467–76.
5. Strobl, G. Crystallization and melting of bulk polymers: new observations, conclusions and a thermodynamic scheme. Progr. Polym. Sci. **2006**, *31*, 398–442.
6. Núñez, E.; Ferrando, C.; Malmström, E.; Claesson, H.; Werner, P.-E.; Gedde, U.W. Crystal structure, melting behaviour and equilibrium melting point of star polyesters with crystallizable poly(ε-caprolactone) arms. Polymer **2004**, *45*, 5251–63.
7. Núñez, E.; Ferrando, C.; Malmström, E.; Claesson, H.; Gedde, U.W. Crystallization behavior and morphology of star polyesters with poly(ε-caprolactone) arms. J. Macromol. Sci. Phys. **2004**, *B43*, 1213–30.
8. Núñez, E.; Gedde, U.W. Single crystal morphology of star-branched polyesters with crystallizable poly(ε-caprolactone) arms. Polymer **2005**, *46*, 5992–6000.
9. Hobbs, J.K.; McMaster, M.J.; Miles, M.J.; Barham, P.J. Direct observations of the growth of spherulites of poly(hydroxybutyrate-*co*-valerate) using atomic-force microscopy. Polymer **1998**, *39*, 2437–2446.
10. Pearce, R.; Vancso, G.J. Imaging of melting and crystallization of poly(ethylene oxide) in real-time by hot-stage atomic-force microscopy. Macromolecules **1997**, *30*, 5843–5848.
11. Claesson, H.; Malmström, E.; Johansson, M.; Hult, A. Synthesis and characterization of star-branched polyesters with dendritic cores and the effect of structural variations on zero shear rate viscosity. Polymer **2002**, *43*, 3511–3518.
12. Ihre, H.; Hult, A.; Söderlind, E. Synthesis, characterization, and ^{1}H-NMR self-diffusion studies of dendritic aliphatic polyesters based on 2,2-bis(hydroxymethyl) propionic acid and 1,1,1-tris(hydroxyphenyl) ethane. J. Am. Chem. Soc. **1996**, *118*, 6388–6395.
13. Blundell, D.J.; Keller, A.; Kovacs, A.J. A self-nucleation phenomenon and its application to the growing of polymer crystals from solution. J. Polym. Sci., Polym. Letters **1966**, *4*, 481–486.
14. Vancso, G.J.; Beekmans, L.G.M.; Pearce, R.; Trifonova, D.; Varga, J. From microns to nanometers: Morphology development in semicrystalline polymers by scanning force microscopy. J. Macromol. Sci., Phys. **1999**, *B38*, 491–500.
15. Wittmann, J.C.; Lotz, B. Polymer decoration: the orientation of polymer folds as revealed by the crystallization of polymer vapors. J. Polym. Sci. Polym. Phys. **1985**, *23*, 205–226.

16. Iwata, T.; Doi, Y. Morphology and enzymatic degradation of poly(ε-caprolactone) single crystals: does a polymer single crystal consist of micro-crystals? Polym. Int. **2002**, *51*, 852–858.
17. Taguchi, K.; Miyamoto, Y.; Mjyaji, H.; Izumi, K. Undulation of lamellar crystals of polymers by surface stresses. Macromolecules **2003**, *36*, 5208–5213.
18. Pouget, E.; Almontassir, A.; Casas, M.T.; Puiggali, J. On the crystalline structures of poly(tetramethylene adipate). Macromolecules **2003**, *36*, 698–705.
19. Organ, S.J.; Hobbs, J.K.; Miles, M.J. Reorganization and melting of polyethylene single crystals: complementary TEM, DSC, and real-time AFM studie. Macromolecules **2004**, *37*, 4562–4572.
20. Winkel, A.K.; Hobbs, J.K.; Miles, M.J. Annealing and melting of long-chain alkane single crystals observed by atomic-force microscopy. Polymer **2000**, *41*, 8791–8800.
21. Beekmans, L.G.M.; van der Meer, D.W.; Vancso, G.J. Crystal melting and its kinetics on poly (ethylene oxide) by in situ atomic-force microscopy. Polymer **2002**, *43*, 1887–1895.
22. Fujita, M.; Doi, Y. Annealing and melting behavior of poly(L-lactic acid) single crystals as revealed by in situ atomic-force microscopy. Biomacromolecules **2003**, *4*, 1301–1307.
23. Harrison, I.R. Polyethylene single crystals: Melting and morphology. J. Polym. Sci., Polym. Phys. **1973**, *11*, 991.
24. Hocquet, S.; Dosiere, M.; Thierry, A.; Lotz, B.; Koch, M.H.J.; Dubreuil, N.; Ivanov, D.A. Morphology and melting of truncated single crystals of linear polyethylene. Macromolecules **2003**, *36*, 8376–8384.
25. Schönherr, H.; Frank, C.W. Ultrathin films of poly(ethylene oxides) on oxidized silicon. 2. In situ study of crystallization and melting by hot stage AFM. Macromolecules **2003**, *36*, 1199–1208.
26. Xu, J.; Guo, B.-H.; Zhang, Z.-M.; Zhou, J.-J.; Jiang, Y.; Yan, S.; Li, L.; Wu, Q.; Chen, G.-Q.; Schultz, J.M. Direct AFM observation of crystal twisting and organization in banded spherulites of chiral poly(3-hydroxybutyrate-co-3-hydroxyhexanoate). Macromolecules **2004**, *37*, 4118–4123.
27. Hobbs, J.K. In *Polymer Crystallization: Observations, Concepts and Interpretations*; Sommer, J.U., Reiter, G., Eds.; Springer-Verlag: Berlin, 2003; 82–95.
28. Organ, S.J.; Keller, A. Solution crystallization of polyethylene at high temperatures. Part 1. Lateral crystal habit. J. Mater. Sci. **1985**, *20*, 1571–1585.
29. Beekmans, L.G.M.; Vancso, G.J. Real-time crystallization study of poly(ε-caprolactone) by hot-stage atomic-force microscopy. Polymer **2000**, *41*, 8975–8981.
30. Godovsky, Yu.K.; Magonov, S.N. Atomic-force microscopy visualization of morphology and nanostructure of an ultrathin layer of polyethylene during melting and crystallization. Langmuir **2000**, *16*, 3549–3552.
31. Li, L.; Chan, C.-M.; Yeung, K.L.; Li, J.-X.; Ng, K.-M; Lei, Y. Direct observation of growth of lamellae and spherulites of a semicrystalline polymer by AFM. Macromolecules **2001**, *34*, 316–325.
32. Kikkawa, Y.; Abe, H.; Fujita, M.; Iwata, T.; Inoue, Y.; Doi, Y. Crystal growth in poly(L-lactide) thin film revealed by in situ atomic-force microscopy. Macromol. Chem. Phys. **2003**, *204*, 1822–1831.